

# THE GALAXY OCTOPOLE MOMENT AS A PROBE OF WEAK LENSING SHEAR FIELDS

DAVID M. GOLDBERG AND PRIYAMVADA NATARAJAN

Department of Astronomy, Yale University, New Haven, CT06511

*Draft version October 25, 2018*

## ABSTRACT

In this paper, we introduce the octopole moment of the light distribution in galaxies as a probe of the weak lensing shear field. While traditional ellipticity estimates of the local shear derived from the quadrupole moment are limited by the width of the intrinsic ellipticity distribution of background galaxies, the dispersion in the intrinsic octopole distribution is expected to be much smaller, implying that the signal from this higher order moment is ultimately limited by measurement noise, and not by intrinsic scatter. We present the computation of the octopole moment and show that current observations are at the regime where the octopole estimates will soon be able to contribute to the overall accuracy of the estimates of local shear fields. Therefore, the prospects for this estimator from future datasets like the Advanced Camera for Survey and the Next Generation Space Telescope are very promising.

*Subject headings:*

## 1. INTRODUCTION

The analysis of weak shear fields of background galaxies lensed by clusters has proved to be a rich field of inquiry (Blandford & Narayan, 1992; Kaiser, Squires & Broadhurst, 1995, hereafter KSB; Kaiser & Squires, 1993; Mellier 1999; Bartelmann & Schneider, 2001 and references therein for applications of weak lensing analysis to observations). However, the underlying assumption of these analyses has always been that all of the lensing information can be extracted from combinations of the quadrupole moments of the light distribution, which define an ellipticity and an orientation for the lensed arclets. Under the assumption that the intrinsic orientation of the lensed galaxy is random, the expectation value of the complex ellipticity can be related to the reduced shear. Do combinations of the quadrupoles contain all the useful information on the local shear field? Refregier & Bacon (2001) point out that any even moment of the light distribution will be preferentially oriented along the shear even in the weak lensing limit.

Moreover, it is generally taken for granted that strong lensing of galaxies, whether producing multiple images or strong arcs, should be analyzed in an fundamentally different way from weakly lensed “arclets”. Kneib et al. (1993), Bartelmann (1995), and others describe the analysis of a strongly lensed arc which lies near a critical curve, and how such images can be used to reconstruct the lens potential.

It is not clear that the transition between arclet and arc is as abrupt as the current mode of analysis would suggest. Another way of thinking about strong arcs is that lensing induces large octopole moments in the light distribution. This octopole has two components: a skewness in the light distribution away from the lens, and a term which expresses itself as an arc tangential to the surface of constant shear. Ideally, there is a transitional regime, one in which the shear is sufficiently weak that the image would not be characterized as an arc, but nevertheless, an octopole moment might be measurable.

The potential benefits of constructing this higher order estimator are significant. Despite the anticipated noisiness of the octopole signal, an optimal combination of this with the quadrupole signal could significantly improve the overall signal to noise, since the absolute value of the intrinsic octopole moments are expected to be small compared to the quadrupole moments. Moreover, since the induced octopole moments implicitly probe the radial variation of the shear field, one may also get an independent local estimate of the radial derivative of the reduced shear.

Forthcoming instruments, such as the Next Generation Space Telescope (NGST), ongoing surveys, including the Deep Lens Survey (DLS), and current and future cluster observations by the Hubble Space Telescope (HST) using the Advanced Camera for Survey, will produce an avalanche of data which need to be fully exploited. The high-quality nature of the data means that the limitation may due to large the number of galaxies (crowded fields making shape measurements tricky) rather than the quality of the imaging, and thus, the octopole approach to data analysis may be quite fruitful.

Our approach in this paper is as follows. The basic lensing formalism of linear distortions and the notation used in this paper are outlined in § 2. In § 3 octopole moments are defined, in the context of them arising from the second-order effects in a circularly symmetric lens. In § 4, the error analysis is discussed, and it is shown that a combination of the quadrupole and octopole can be used to estimate the reduced shear and its spatial derivative. Finally, in § 5, we present a discussion of future prospects, including application to observational data-sets.

## 2. BACKGROUND

We begin by defining our convention and reminding the reader of the standard weak lensing equations. An excellent and exhaustive review of this material can be found in Bartelmann & Schneider (2001), from which our conventions are borrowed.

A point mass,  $M$ , at a distance,  $D_l$ , will deflect a light beam coming from a source at distance,  $D_s$ . In particular, if the source is observed at a 2-d angle  $\vec{\theta}$  from the lens, then the beam would be deflected by an angle,  $\vec{\alpha}$ :

$$\vec{\alpha}_{PS} = \frac{(D_l - D_s)D_l}{D_s} \frac{4GM}{c^2\theta} \hat{\theta}. \quad (1)$$

More generally, if the lens is an extended object, with a surface mass density,  $\Sigma(\vec{\theta})$ , then a dimensionless mass, the convergence, may be defined as:

$$\kappa(\vec{\theta}) = \frac{\Sigma(\vec{\theta})}{\Sigma_{cr}} \equiv \frac{(D_l - D_s)D_l}{D_s} \frac{4\pi G \Sigma(\vec{\theta})}{c^2}. \quad (2)$$

The convergence may be thought of as a source term for a potential,  $\psi(\vec{\theta})$ , and related via a Poisson-like equation:

$$\nabla^2 \psi(\vec{\theta}) = 2\kappa(\vec{\theta}), \quad (3)$$

where all gradients and divergences are calculated in the two-dimensional  $\theta$ -space.

Extension of equation (1) to the continuous case, and combination with equation (2) yields a deflection angle,

$$\vec{\alpha}(\vec{\theta}) = \frac{1}{\pi} \int d^2\vec{\theta}' \kappa(\vec{\theta}') \frac{\vec{\theta} - \vec{\theta}'}{|\vec{\theta} - \vec{\theta}'|^2}. \quad (4)$$

A beam observed at angle  $\vec{\theta}$  must therefore have originated in the source plane at

$$\vec{\beta}(\vec{\theta}) = \vec{\theta} - \vec{\alpha}(\vec{\theta}), \quad (5)$$

under the thin lens approximation.

Suppose we observe a galaxy with its center of light at the position  $\vec{\beta}_0$  *in the source plane*. Throughout this paper, we will define a local set of coordinates such that  $\vec{\beta}_0$ , and correspondingly,  $\vec{\theta}_0$  (the position of the source in the lens plane) are at the origin. This assumed convention does not change the final results, but merely makes the equations more compact. Solving the lensing equation to linear order, one finds that both  $\vec{\beta}_0$  and  $\vec{\theta}_0$  correspond to the center of mapping (i.e. the first order lens mapping from source plane to image plane preserves the position of the center of light).

In linear analysis both  $\vec{\beta}_0$  and  $\vec{\theta}_0$  correspond to the center of light. However, in the higher order analysis, discussed below, if the position,  $\vec{\beta}_0$ , in the source plane is lensed to the foreground, the corresponding lensed position will no longer necessarily be the center of light.

Combining equations (2) & (3), the deflection angle,  $\vec{\alpha}(\vec{\theta})$  can be written explicitly as the gradient of the scalar potential,  $\vec{\alpha}(\vec{\theta}) \equiv \nabla_{\vec{\theta}} \psi$ . Since lensing conserves surface brightness, a mapping from foreground to background coordinates is sufficient to determine a background brightness map from a foreground one (or vice-versa) provided a full knowledge of the geometry of the system (cosmology plus the redshifts of the source and lens) and mass distribution of the lens. Thus, we may expand around the origin to determine a deprojection operator on a foreground light distribution, which yields the amplification matrix,

$$\mathbf{A}(\vec{\theta}) \equiv \frac{\partial \vec{\beta}}{\partial \vec{\theta}} = \left( \delta_{ij} - \frac{\partial^2 \psi(\vec{\theta})}{\partial \theta_i \partial \theta_j} \right) \equiv \begin{pmatrix} 1 - \kappa - \gamma_1 & -\gamma_2 \\ -\gamma_2 & 1 - \kappa + \gamma_1 \end{pmatrix}. \quad (6)$$

Rigorously speaking, this expression is the first term in a Taylor series expansion of the distortion operator. The term  $\gamma$  is a complex shear term, representing the anisotropic part of the distortion, with  $\gamma = |\gamma|e^{2i\phi}$ , and the real and imaginary parts being denoted with the subscripts, “1” and “2” respectively, as per convention. Using our locally defined coordinate system, we have:

$$\beta_i = \mathbf{A}_{ij} \theta_j \quad (7)$$

Likewise, assuming the absence of a caustic crossing ( $1 - \kappa - |\gamma| < 0$ ), this can be inverted uniquely to give a projection function,

$$\theta_i = \mathbf{A}_{ij}^{-1} \beta_j \quad (8)$$

In this analysis, we focus on expanding this projection operator to the next higher order to derive the octopole moment rather than restricting ourselves to the quadrupole moment alone. In general, researchers have treated weak lensing fields in the manner described by KSB or its variants (Bacon, Refregier & Ellis, 2000; van Waerbeke et al. 2001). These techniques describe the mapping of source-plane quadrupole light distributions to lens-plane distributions, and thus use the observed ellipticity and an assumption of random orientation to invert the shear field. In this work, we aim to generalize these transformations to the next higher order. Our notation for the  $n$ -th order moments of a galaxy is:

$$\langle x^n y^m \rangle \equiv \frac{\int dx dy I(x, y) (x - \bar{x})^n (y - \bar{y})^m}{\int dx dy I(x, y)}, \quad (9)$$

where an overline indicates the mean value, where for the quadrupole  $n + m = 2$ . We may redefine the surface brightness,  $I(x, y)$  to any other function of flux without a loss of generality in the above expression.

The quadrupole moments are generally translated into a complex ellipticity via one of the relations:

$$\epsilon = \frac{\langle x^2 \rangle - \langle y^2 \rangle + 2i\langle xy \rangle}{\langle x^2 \rangle + \langle y^2 \rangle + 2\sqrt{\langle x^2 \rangle \langle y^2 \rangle - \langle xy \rangle^2}} \quad (10)$$

or

$$\chi = \frac{\langle x^2 \rangle - \langle y^2 \rangle + 2i\langle xy \rangle}{\langle x^2 \rangle + \langle y^2 \rangle} \quad (11)$$

The expectation value of the complex ellipticities around a circular annulus gives an estimate of the combination of parameters:

$$E(\epsilon_\theta) \simeq g \equiv \frac{\gamma}{1 - \kappa} , \quad (12)$$

$$E(\chi_\theta) \simeq 2g \quad (13)$$

where  $g$  is known as the reduced shear. This expression implies a degeneracy between values of the shear and convergence. It should also be noted that these relations hold only in the limit of small variance in the intrinsic ellipticity distribution and for small values of  $g$ . Strictly speaking, these approximations are invalid in the strong lensing regime characterized by the dramatic arcs and multiple images.

### 3. THE OCTOPOLE MOMENTS

In this section, we address the issue of analysis of higher order moments of the light distribution. In particular, we show that, even in the weak lensing limit in which one would strictly not expect to be able to detect gravitational arcs, an arc-like signature can be found from the octopole moments of the galaxy light distribution.

In order to simplify this discussion somewhat, we assume a radially symmetric potential throughout, and for a fiducial galaxy we further choose the coordinate system with a configuration such that it lies along the positive x-axis. This is entirely equivalent to defining a radial and tangential component. However, for practical reasons, we chose to do all calculations in Cartesian coordinates.

Under these assumptions, using only linear theory, the lensed (subscript  $\theta$ ) and unlensed (subscript  $\beta$ ) moments can be related in a very straightforward way since the Jacobian is diagonal. Thus,

$$\langle x^n y^m \rangle_\theta = [A_{11}^{-1}]^n [A_{22}^{-1}]^m \langle x^n y^m \rangle_\beta = \frac{1}{(1 - \kappa - \gamma)^n} \frac{1}{(1 - \kappa + \gamma)^m} \langle x^n y^m \rangle_\beta . \quad (14)$$

Application of this transform to the quadrupole terms in the weak lensing limit, yields the complex ellipticity transformations above. If galaxies are randomly oriented, as is assumed (however, see Crittenden et al. 2001 for an estimate of the degree of expected intrinsic alignments), then the expectation value of any of the intrinsic octopole moments (and hence the lensed octopole moments in a circularly symmetric potential) will necessarily vanish.

However, even in the absence of an intrinsic octopole moment, the second order Taylor expansion of the lensing equation can give rise to octopole moments. Consider the limit when the source image has a small but finite size, the lensed field may be approximated as:

$$\beta_i \simeq A_{ij} \theta_j + \frac{1}{2} A_{ij,k} \theta_j \theta_k . \quad (15)$$

By inspection, the following symmetries:  $A_{ik,j} = A_{ij,k}$  and  $A_{ji,k} = A_{ij,k}$ , hold. The corresponding terms (expressible as local derivatives of the shear and convergence field) are:

$$\begin{aligned} A_{11,1} &= -\kappa_{,1} - \gamma_{1,1} = -2\gamma_{1,1} - \gamma_{2,2} = -2\gamma_{1,1} - \frac{2\gamma}{r} = -2\gamma' - \frac{2\gamma}{r} \\ A_{12,1} &= A_{21,1} = A_{11,2} = -\gamma_{2,1} = 0 \\ A_{22,1} &= A_{12,2} = A_{21,2} = -\kappa_{,1} + \gamma_{1,1} = -\gamma_{2,2} = -\frac{2\gamma}{r} \\ A_{22,2} &= -\kappa_{,2} + \gamma_{1,2} = 0 , \end{aligned} \quad (16)$$

where  $\gamma' = \partial\gamma/\partial r$ , the radial derivative of the shear field.

Since the potential, and thus the surface density of the lens,  $\Sigma(\vec{\theta})$ , is circularly symmetric, and the center of the lens lies on the x-axis,  $\kappa_{,2} = 0$ . Likewise, since everywhere on the x-axis,  $\gamma_2 = 0$ ,  $\gamma_{2,1} = 0$ . In addition, we have used the relation derived by Kaiser (1995):

$$\begin{pmatrix} \kappa_{,1} \\ \kappa_{,2} \end{pmatrix} = \begin{pmatrix} \gamma_{1,1} + \gamma_{2,2} \\ \gamma_{2,1} - \gamma_{1,2} \end{pmatrix} . \quad (17)$$

Finally, it can be shown that  $\gamma_{2,2} = 2\gamma/r$ .

Summarizing and incorporating all the above symmetries and simplifications, we have:

$$\begin{aligned} x_\beta &\simeq A_{11}x_\theta - \left[\gamma' + \frac{\gamma}{r}\right] x_\theta^2 - \frac{\gamma}{r} y_\theta^2 \\ y_\beta &\simeq A_{22}y_\theta - \frac{2\gamma}{r} x_\theta y_\theta \end{aligned} \quad (18)$$

Thus, to second order in the position, the above equations may be inverted:

$$\begin{aligned} x_\theta &\simeq A_{11}^{-1}x_\beta + A_{11}^{-3} \left[\gamma' + \frac{\gamma}{r}\right] x_\beta^2 + A_{11}^{-1}A_{22}^{-2} \frac{\gamma}{r} y_\beta^2 \\ y_\theta &\simeq A_{22}^{-1}y_\beta + A_{11}^{-1}A_{22}^{-2} \frac{2\gamma}{r} x_\beta y_\beta . \end{aligned} \quad (19)$$

In order to compute the moments of the lensed field, we need to transform the area element by determining the Jacobian consistently to the same order,

$$\begin{aligned} J &\equiv \left| \frac{\partial x_\theta}{\partial x_\beta} \frac{\partial y_\theta}{\partial y_\beta} \right| \\ &= \left| \begin{array}{cc} A_{11}^{-1} + 2A_{11}^{-3} \left[\gamma' + \frac{\gamma}{r}\right] x_\beta & 2A_{11}^{-1}A_{22}^{-2} \frac{\gamma}{r} y_\beta \\ 2A_{11}^{-1}A_{22}^{-2} \frac{\gamma}{r} y_\beta & A_{22}^{-1} + 2A_{11}^{-1}A_{22}^{-2} \frac{\gamma}{r} x_\beta \end{array} \right| \\ &\simeq \mu + \left( 2A_{11}^{-3}A_{22}^{-1} \left[\gamma' + \frac{\gamma}{r}\right] + 2A_{11}^{-2}A_{22}^{-2} \frac{\gamma}{r} \right) x_\beta , \end{aligned} \quad (20)$$

to first order in  $x_\beta$ . This yields an area element in the lensed field such that  $dx_\theta dy_\theta = J dx_\beta dy_\beta$ .

We may now compute the expected transformation of any given moment. The total flux,  $f$  from the galaxy, for example is:

$$f_\theta = \int I(x, y) J dx_\beta dy_\beta = \mu f_\beta \quad (21)$$

which is precisely the result in linear theory. We may also compute the shift in the center of light compared to the linear theory prediction. Symmetry arguments, along with our choice of coordinates clearly will produce no shift in the y-coordinate direction.

However,

$$\begin{aligned} \langle x \rangle_\theta &= \frac{1}{\mu f_\beta} \int \left( A_{11}^{-1}x_\beta + A_{11}^{-3} \left[\gamma' + \frac{\gamma}{r}\right] x_\beta^2 + A_{11}^{-1}A_{22}^{-2} \frac{\gamma}{r} y_\beta^2 \right) J dx_\beta dy_\beta \\ &= \left[ 3A_{11}^{-3} \left(\gamma' + \frac{\gamma}{r}\right) + 2A_{11}^{-2}A_{22}^{-1} \frac{\gamma}{r} \right] \langle x^2 \rangle_\beta + A_{11}^{-1}A_{22}^{-2} \frac{\gamma}{r} \langle y^2 \rangle_\beta \\ &= \left[ 3A_{11}^{-1} \left(\gamma' + \frac{\gamma}{r}\right) + 2A_{22}^{-1} \frac{\gamma}{r} \right] \langle x^2 \rangle_\theta + A_{22}^{-1} \frac{\gamma}{r} \langle y^2 \rangle_\theta \end{aligned} \quad (22)$$

Since this shift merely reflects a change in position between the first and second order approximation of the lensing inversion, it is not directly measurable. On the other hand, we may compute the expectation values of the observables,  $\langle x^3 \rangle_\theta$  and  $\langle xy^2 \rangle_\theta$ :

$$\begin{aligned} \langle x^3 \rangle_\theta &= A_{11}^{-3} \langle x^3 \rangle_\beta + \left[ 2A_{22}^{-1} \frac{\gamma}{r} + 5A_{11}^{-1} \left(\gamma' + \frac{\gamma}{r}\right) \right] \langle x^4 \rangle_\theta + 3A_{11}^{-1} \frac{\gamma}{r} \langle x^2 y^2 \rangle_\theta \\ &\quad - \left[ 9A_{11}^{-1} \left(\gamma' + \frac{\gamma}{r}\right) + 6A_{22}^{-1} \frac{\gamma}{r} \right] \langle x^2 \rangle_\theta^2 - 3A_{11}^{-1} \frac{\gamma}{r} \langle x^2 \rangle_\theta \langle y^2 \rangle_\theta^2 \\ &= A_{11}^{-3} \langle x^3 \rangle_\beta + \left[ 2 \frac{g}{r(1+g)} + 5 \left( \frac{g' - g/r - g^2/r}{1 - g^2} \right) \right] \langle x^4 \rangle_\theta + 3 \frac{g}{r(1-g)} \langle x^2 y^2 \rangle_\theta \\ &\quad - \left[ 9 \left( \frac{g' - g/r - g^2/r}{1 - g^2} \right) + 6 \frac{g}{r(1+g)} \right] \langle x^2 \rangle_\theta^2 - 3 \frac{g}{r(1-g)} \langle x^2 \rangle_\theta \langle y^2 \rangle_\theta^2 \end{aligned} \quad (23)$$

and

$$\begin{aligned} \langle xy^2 \rangle_\theta &= A_{11}^{-1}A_{22}^{-2} \langle xy^2 \rangle_\beta + \left[ 3A_{11}^{-1} \left(\gamma' + \frac{\gamma}{r}\right) + 6A_{22}^{-1} \frac{\gamma}{r} \right] \langle x^2 y^2 \rangle_\theta + A_{11}^{-1} \frac{\gamma}{r} \langle y^4 \rangle_\theta \\ &\quad - \left[ 3A_{11}^{-1} \left(\gamma' + \frac{\gamma}{r}\right) + 2A_{22}^{-1} \frac{\gamma}{r} \right] \langle x^2 \rangle_\theta \langle y^2 \rangle_\theta - A_{11}^{-1} \frac{\gamma}{r} \langle y^2 \rangle_\theta^2 \\ &= A_{11}^{-1}A_{22}^{-2} \langle xy^2 \rangle_\beta + \left[ 3 \left( \frac{g' - g/r - g^2/r}{1 - g^2} \right) + 6 \frac{g}{1+g} \right] \langle x^2 y^2 \rangle_\theta + \frac{g}{1+g} \langle y^4 \rangle_\theta \\ &\quad - \left[ 3 \left( \frac{g' - g/r - g^2/r}{1 - g^2} \right) + 2 \frac{g}{1+g} \right] \langle x^2 \rangle_\theta \langle y^2 \rangle_\theta - \frac{g}{1-g} \langle y^2 \rangle_\theta^2 \end{aligned} \quad (24)$$

In both these expressions (eqns. 23 and 24), the terms proportional to squares of the quadrupole moments arise from a second order shift in the center of light. By inspection, the expectation values of the other two octopole moments,  $\langle x^2 y \rangle_\theta$  &  $\langle y^3 \rangle_\theta$ , will vanish.

Note that with the exception of the term proportional to the intrinsic octopole moments, both the lensed octopoles are a function of observables: the second and fourth moments of the light, the reduced shear,  $g$ , and its first derivative. The octopole analysis, however, retains the degeneracy found in quadrupole analysis. However, since the scatter in the intrinsic octopoles may be much smaller than the scatter in the intrinsic ellipticity, and since it has a mean of zero, extracting a profile of  $g(r)$  from a finite number of noisy galaxies may be done with potentially higher signal to noise by using the third as well as the second moments. We discuss this parameter extraction in the next section.

#### 4. ERROR ANALYSIS AND PARAMETER ESTIMATION

##### 4.1. Estimation of the Errors on the Moments

The fact that lensing induces an octopole moment in an otherwise elliptical galaxy is interesting, but by no means useful unless we are actually able to measure this effect. We must measure both the octopole moments and the hexadecipole moments with some accuracy in order to extract the shear, and since both moments are much more likely to be contaminated by sky noise than their quadrupole counterparts, it is possible that measuring these moments may be quite difficult. In order to estimate the feasibility of such an investigation, we must first consider the uncertainties in measuring the moments for a fiducial galaxy.

We make a number of simplifying assumptions in estimating the moment uncertainties. First, we assume that the only source of error arises from the Poisson noise in the galaxy image and the background sky. We thus do not include the effects of a PSF, which are likely to be considerably more important on the lower order quadrupole moments than on the octo- and hexadecipoles. Similarly, we do not include pixelation effects, which are also expected to be more important for the quadrupoles. However, we do assume that the background sky level is constant (up to Poisson noise) over the entire image, and that the galaxy image is unblended with any of its neighbors. It is these effects that will contribute significantly to the noise in the higher order moments.

Given these constraints, we assume that a good estimate of the moments of a galaxy can be achieved by integrating using a circular mask, including a tophat and Gaussian. Although, this is clearly not optimal, as a circular mask will introduce biases in all moments, we adopt this aperture for purposes of illustration in this work. The generality of the formalism developed here allows one to potentially replace the surface brightness in equation (9), with any other monotonic function of surface brightness. However, optimal determination of this function would rely on some knowledge of the true radial light profile of the galaxy.

Clearly, the analysis can be successfully performed for an elliptical mask, or even an arbitrarily shaped mask, in which instance the relevant region above some given isophote could be determined iteratively. Discussion and application of optimal shape estimation can be found in the literature on IMCAT (Kaiser), sExtractor (Bertin & Arnouts, 1996), FOCAS (Jarvis & Tyson 1981). However, these pieces of software have focused on estimating only the ellipticity and other shape parameters related to the quadrupole moments.

Specially promising among recent shape estimation methods is the Shapelets technique (Refregier & Bacon, 2001; Refregier, 2001) which decomposes images into Hermite polynomial basis sets. A potential approach to computing octopole moments may be to determine the second order shear operator directly in shapelet space.

However, it is beyond the scope of the analysis of this work to investigate optimal techniques for measuring higher order moments. This will be dealt with in future work. For the present, we will simply use the assumptions above to effectively characterize the practical measurement uncertainties in typical images.

That said, one may approximate the uncertainty in  $\langle x^n y^m \rangle$ ,  $\sigma_{n,m}$  as:

$$\sigma_{n,m}^2 \simeq \frac{\int_0^{2\pi} d\theta \cos^{2n}(\theta) \sin^{2m}(\theta) \int_0^\infty dr w^2(r, \theta) r^{1+2n+2m} [I(r, \theta) + N]}{\left( \int_0^{2\pi} d\theta \int_0^\infty dr w(r, \theta) r I(r, \theta) \right)^2}, \quad (25)$$

where  $I(r, \theta)$  is the surface brightness in counts/area of the galaxy,  $N$  is the background sky brightness in counts/area, and  $w(r, \theta)$  is a mask. For our analysis, we use two forms for this mask, a tophat, with  $w = 1$  out to a specified outer radius, and a circular Gaussian, as used in KSB.

The form of the integral explicitly assumes that the light is very nearly circularly distributed. For an assumed radial profile, the error may be approximated analytically or semi-analytically. For our analysis, we have used a de Vaucouleurs (1948) profile:

$$I(r, \theta) = I_e \exp\{-7.67[(R/R_e)^{1/4} - 1]\}, \quad (26)$$

where  $I_e$  is the characteristic brightness, and  $R_e$  is the half light radius. We find similar error estimates for other assumed profiles. Typically, we set the outer radius at 4 times the half-light radius.

Note that we ignore any covariances in the errors. While inclusion of these terms in our analysis would generally lower the implied errors, their effect is expected to be small compared to other uncertainties which we have explicitly overlooked.

In addition to measurement errors, both the ellipticity estimate of the shear and the octopole measurement of the shear require an estimate of the intrinsic scatter of the ellipticity or the octopole. The first we will label  $\sigma_\chi$ , which is somewhat

different from the value normally given. Since we assume a random orientation,  $\sigma_\chi$  represents the standard deviation in the intrinsic distribution of the real part of the complex ellipticity, a term which has an expected mean of zero.

The intrinsic variation in the octopole moments in the octopoles are labeled  $\sigma_{\langle x^3 \rangle}$ , and  $\sigma_{\langle xy^2 \rangle}$ . These terms represent the standard deviation in the following dimensionless form:

$$\sigma_{\langle x^3 \rangle}^3 = \left\langle \left( \frac{\langle x^3 \rangle}{R_e^3} \right)^2 \right\rangle^{1/2}, \quad (27)$$

with a similar form for the other octopole. We again assume no covariance.

To simplify the analysis, we assume that the half-light radius,  $R_e$ , and the characteristic radius is known with perfect certainty, as is the integrated flux. Since these terms are dominant near the center of the image, their errors will be considerably smaller than the higher order moments.

#### 4.2. Uncertainty from Ellipticity Estimates

Finally, we consider the uncertainty in the shear from the measurement of the quadrupoles of a single galaxy. In the limit of weak lensing, the reduced shear may be approximated as:

$$g \simeq \frac{\chi_1 - \chi_1^{(s)}}{2} = \frac{\langle x^2 \rangle - \langle y^2 \rangle}{2r_0^2} - \frac{\chi_1^{(s)}}{2}. \quad (28)$$

Since the orientation of the intrinsic ellipticity,  $\chi_\beta$  is random,  $\sigma_{\chi_1} = \sigma_\chi / \sqrt{2}$ . Ebbels et al. (2000) derive a probability distribution function for the observed ellipticity distribution for galaxies of different morphological types from the Medium Deep Survey. Adapting this, we find a reasonable value of  $\sigma_\chi = 0.30$ .

Thus, the variance in the estimate of  $g$  from the ellipticity is:

$$\sigma_{g-Q}^2 \simeq \frac{\sigma_{2,0}^2 + \sigma_{0,2}^2}{4r_0^4} + \frac{\sigma_\chi^2}{4} \quad (29)$$

In most instances, this uncertainty will be dominated by the spread in the intrinsic galaxy ellipticities.

#### 4.3. Uncertainty from Octopole Estimates

The details of parameter estimation from the octopole moments are slightly more involved. We may begin by simplifying the terms in eqns. (24 and 25) which are functions of  $g$ . For small  $g$ , we may say:

$$\frac{g}{(1+g)} \simeq g \quad ; \quad \frac{rg' - g - g^2}{1 - g^2} \simeq rg' - g \quad (30)$$

We then simplify eqns. (24 and 25) to the following expressions:

$$\langle x^3 \rangle_\theta = A_{11}^{-3} \langle x^3 \rangle_\beta + u_{11}g + u_{12}r g', \quad (31)$$

and

$$\langle xy^2 \rangle_\theta = A_{11}^{-1} A_{22}^{-2} \langle xy^2 \rangle_\beta + u_{21}g + u_{22}r g', \quad (32)$$

where the terms,  $u_{ij}$ , can be derived by inspection, and their uncertainties can be determined by the standard propagation of errors. We reiterate here that this analysis assumes that the errors are Gaussian and uncorrelated, which is certainly not the case.

Inverting these expressions yields:

$$g \simeq \frac{1}{u_{11}u_{22} - u_{12}u_{21}} [u_{22}(\langle xy^2 \rangle_\theta - A_{11}^{-1} A_{22}^{-2} \langle xy^2 \rangle_\beta) - u_{12}(\langle x^3 \rangle_\theta - A_{11}^{-3} \langle x^3 \rangle_\beta)] \quad (33)$$

and

$$r g' \simeq \frac{1}{u_{11}u_{22} - u_{12}u_{21}} [-u_{21}(\langle xy^2 \rangle_\theta - A_{11}^{-1} A_{22}^{-2} \langle xy^2 \rangle_\beta) + u_{11}(\langle x^3 \rangle_\theta - A_{11}^{-3} \langle x^3 \rangle_\beta)] \quad (34)$$

Since the expectation value of the intrinsic octopoles is zero, estimating the parameters from these equations is straightforward.

Finally, from the form above, calculation of the variance and covariance of  $g$  and  $r g'$  is a straightforward but tedious exercise in propagation of errors.

## 4.4. Results

It now remains for us to compare errors estimated from the quadrupole moments alone to those from the octopole moments. For these estimates, we assume the galaxy to intrinsically follow a de Vaucouleurs profile. Note that this assumption is necessary only in computing the estimate of the error, and is not required for parameter estimation.

The fiducial galaxy has a magnitude of 22 at  $z = 0.5$ , and has a half-light radius in the source plane of 2kpc. Error estimates are made for observations taken using the HST Wide Field camera using a 16.8 ks exposure as was used for observations of AC114 (Natarajan et al. 1998). Signal and sky counts were estimated using the HST WFPC2 exposure time calculator<sup>1</sup>. The lens and source are separated by 100 pixels in the image, and we take a fiducial shear of 2% at the center of the source. The lens is assumed to be isothermal, with 2% mean shear at that radius. The precise amplitude of the shear is not that important in comparing the ellipticity and octopole estimate error bars, since both techniques are, in fact, first order in the shear.

The deviation in the intrinsic ellipticity,  $\sigma_\chi$  is taken as 0.30, as discussed above while the scatter in both the intrinsic octopoles is 0.1. The intrinsic octopole distribution is not well studied, and understanding this may prove to be a fruitful inquiry into galaxy shapes. We select a very small scatter here for the following reason. If the intrinsic dispersion in the octopole moments is sufficiently large that for most observational sets the uncertainties in parameter estimation are dominated not by photon Poisson noise, but by shot noise in the sample, then the octopole moment at best improves the signal to noise compared to the quadrupole by  $\sqrt{2}$ . The transition from Poisson to shot noise domination is illustrated in Fig. 2g.

The error ellipses from the quadrupole and octopole estimates of  $g$  and  $rg'$ , along with their combined ellipse can be found in Figure 1. Note that even for existing data sets, inclusion of the octopole analysis has the potential to yield significant new information about the shear field.

The effect of the choice of physical and observational parameters on the estimated errors are shown in Figure 1. The error ellipses for a slice through parameter space are shown in Figure 2. Analysis is performed using a Gaussian mask with an effective radius equal to the half light radius.

Note that variations in the observational and physical parameters within these ranges do not generally alter the error from the quadrupole moment alone. This is because in this regime, the quadrupole error is dominated by the intrinsic

<sup>1</sup>[http://www.stsci.edu/instruments/wfpc2/Wfpc2\\_etc/wfpc2-etc.html](http://www.stsci.edu/instruments/wfpc2/Wfpc2_etc/wfpc2-etc.html)

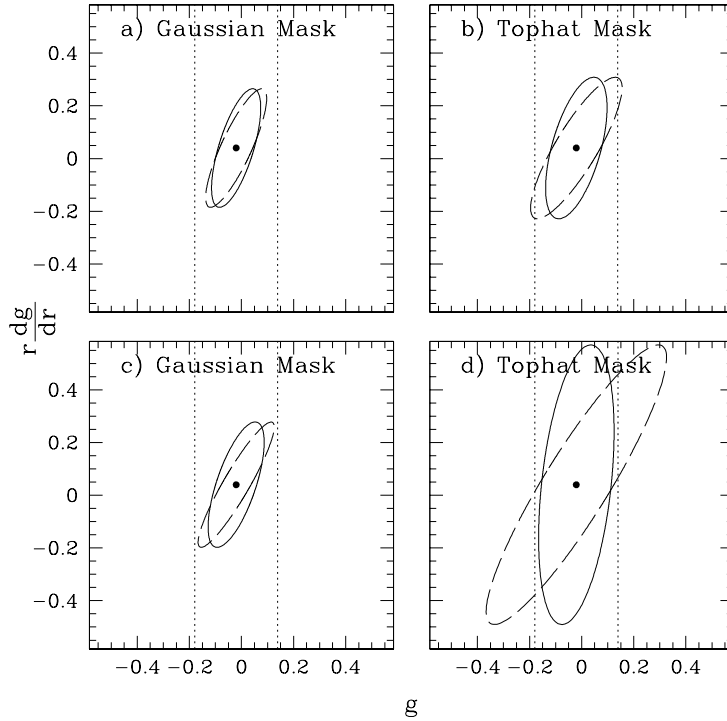


FIG. 1.— The calculated error ellipses using the method developed in this paper. The dotted lines represent the  $1\sigma$  errors on  $g$  from the quadrupole technique alone. The dashed line represents the  $1 - \sigma$  error ellipse on  $g$  and  $rg'$  from the octopole method. The solid ellipse is the combined error estimate. In each panel, the simulated galaxy has been assigned an apparent magnitude of 22 at  $z = 0.5$ . Calculations are done for the HST Wide Field Camera using the 814nm filter. Exposure time is set for 16.8ks,  $\sigma_\chi = 0.30$ , and the relative variances for both relevant octopole moments are set to 0.1. The reduced shear is set to 2%, and the source appears 100 pixels from the lens. The four panels use different masks to do the signal to noise estimate. Panels a) and c) use Gaussian masks, as described in KSB, with characteristic radii set to the  $R_e$  and  $2R_e$ , respectively. Panels b) and d) use tophat masks, with radii equal to  $2R_e$  and  $4R_e$ , respectively.

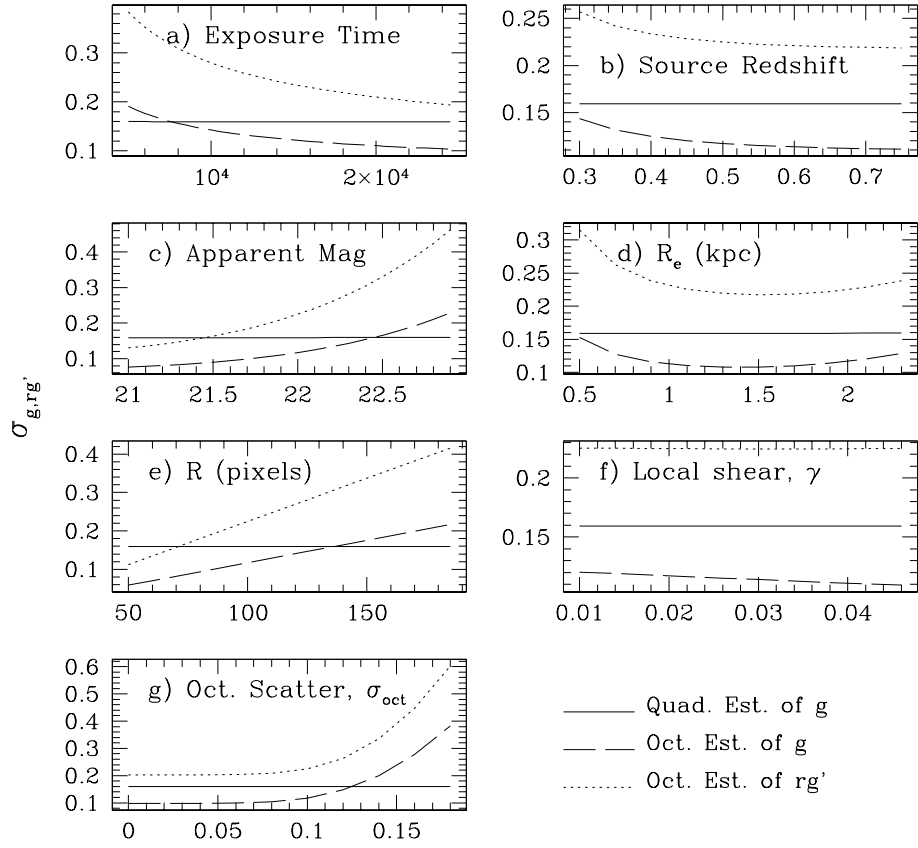


FIG. 2.— A sequence of slices through observational and physical parameters, comparing the variation of uncertainty in parameter estimates. We vary a) exposure time, b) source redshift, c) source apparent magnitude, d) source effective radius, e) source-lens separation on the chip, f) local shear on the source, and g) intrinsic scatter in the octopole. Note that the uncertainty in  $g$  arising from the quadrupole estimate alone remains essentially unchanged over this set of parameters. This is due to the fact that within this regime the dominant effect in the quadrupole signal is produced by shot noise.



variation in ellipticities, rather than measurement errors. If such is the case, then we are necessarily limited by shot noise in the number of sources rather than Poisson noise. If the intrinsic scatter in the octopole moment is sufficiently large, this may be the case for the octopole estimator as well. However, we reiterate that this statistic is not well-studied.

For brighter sources or longer exposures, the quality of estimates for the octopoles improves quickly, as do the estimates if the distance to the lens decreases, even if this is not accompanied by a corresponding increase in local shear.

## 5. DISCUSSION AND FUTURE PROSPECTS

In this paper, we have introduced a new and potentially powerful way of analyzing weak lensing shear fields – using the octopole moments of the observed light distribution as a second-order estimator of the shear. In addition to the shear, we also obtain an estimate of its radial derivative. The radial derivative of the shear field provides an important constraint on the mass profiles of the dark matter halos that host galaxies. There are few other methods that can probe that variation.

While we have demonstrated that within the range of reasonable physical and observational parameters the corresponding measurement uncertainties for the octopole may be comparable to those found using traditional ellipticity estimates of the shear, much remains to be done, both theoretically and observationally. The Gaussian mask used in estimating the octopole and quadrupole moments is almost certainly not optimal for this technique. In order to apply this to observations, shape estimators must be used which can compute these higher-order moments with maximum signal to noise. One avenue of inquiry is to apply a second-order analysis to the Shapelet (Refregier, 2001; Refregier & Bacon, 2001) technique in order to get a comparable signal.

In addition, we have created a somewhat simplistic model of the lens as a circular system. Schneider & Bartelmann (1997), for example, consider an extension of KSB with an elliptical lens. Such an effect would introduce an additional degree of freedom in the present analysis, since the shear and its radial derivative would no longer necessarily align. Application of this technique with generality must include these effects.

Finally, this technique needs to be applied to data. A number of excellent observational datasets exist with comparable observational parameters to those used in the text (e.g. AC114, Natarajan et al. 1998). In addition, the Deep Lens Survey<sup>2</sup> (DLS), and the forthcoming HST Advanced Camera for Survey (ACS) will provide the sort of high-quality data which will be ideal for this analysis. We hope to present an application to currently available data-sets in a future paper. It is clear that there is significant information in higher-order moments of the light distribution of galaxies, beyond just the ellipticity, and here we have illustrated the uses of the octopole moment.

We would like to thank Ue-Li Pen and Tereasa Brainerd for helpful discussions.

## REFERENCES

- |  |   |
|--|---|
| Bacon, D.J., Refregier, R., & Ellis, R.S., 2000, MNRAS, 318, 625   | Kneib, J-P., Meiller, Y., Fort, B. & Mathez, G., 1993, A&A, 273, 367  |
| Bartelmann, M. 1995, A&A, 299, 11  | Mellier, Y., 1999, ARA&A, 37, 127   |
| Bartelmann, M. & Schneider, P., 2001, Phys. Rep., 340, 291   | Natarajan, P., Kneib, J.-P., Smail, I. & Ellis, R.S., 1998 ApJ, 499, 600  |
| Bertin, E. & Arnouts, S., 1996, A&AS 117, 393  | Refregier, A. & Bacon, D. 2001, submitted to MNRAS, preprint at <a href="http://xxx.lanl.gov/abs/astro-ph/0105179">http://xxx.lanl.gov/abs/astro-ph/0105179</a> |
| Blandford, R.D. & Narayan, R. 1992, ARA&A, 30, 311   | Refregier, A. 2001, submitted to MNRAS, preprint at <a href="http://xxx.lanl.gov/abs/astro-ph/0105178">http://xxx.lanl.gov/abs/astro-ph/0105178</a>             |
| de Vaucouleurs, G. 1948, AA, 11, 247   | Schneider, P. & Bartelmann, M., 1997, MNRAS, 286, 696   |
| Ebbels, T. et al., 2000, in prep.  | van Waerbeke et al., 2001, A&A, 358, 30   |
| Jarvis, J.F. & Tyson, J.A. 1981, AJ, 86, 476   |   |
| Kaiser, N. 1995, ApJL, 439, 1  |   |
| Kaiser, N. & Squires, G. 1993, ApJ, 404, 441   |   |
| Kaiser, N., Squires, G., & Broadhurst, T. 1995, ApJ, 449, 460  |   |
| Kaiser, N. <a href="http://www.ifa.hawaii.edu/~kaiser/imcat/man/imcat.html">http://www.ifa.hawaii.edu/~kaiser/imcat/man/imcat.html</a> (IMCAT) |   |

<sup>2</sup><http://dls.bell-labs.com>